

DEVELOPMENT OF RADIATION MEDICINE AT DLNP, JINR

*E. M. Syresin, A. V. Agarov, N. V. Anfimov, G. A. Chelkov, V. N. Gaevsky,
V. G. Elkin, G. A. Karamysheva, M. Yu. Kazarinov, N. N. Khovansky,
S. A. Kostromin, V. G. Kruchonok, Z. V. Krumshstein, E. I. Luchin, G. V. Mitsyn,
A. G. Molokanov, N. A. Morozov, A. G. Olshevsky, V. M. Romanov,
Z. Ya. Sadygov, E. V. Samsonov, A. S. Selyunin, N. G. Shakun, K. N. Shipulin,
G. D. Shirkov, S. V. Shvidky, A. S. Zhemchugov*

Joint Institute for Nuclear Research, Dubna

V. A. Novikov, O. P. Tolbanov, A. V. Tyazhev

Academician V. D. Kouznetsov Siberian Physical and Technical Institute, Tomsk State University,
Tomsk, Russia

Y. Jongen

Ion Beam Application, Louvain-la-Neuve, Belgium

The Dzhelapov Laboratory of Nuclear Problems' activity is aimed at developing three directions in radiation medicine: 3D conformal proton therapy, accelerator techniques for proton and carbon treatment of tumors, and new types of detector systems for spectrometric computed tomography (CT) and positron emission tomography (PET).

JINR and IBA have developed and constructed the medical proton cyclotron C235-V3. At present, all basic cyclotron systems have been built. We plan to assemble this cyclotron at JINR in 2011 and perform tests with the extracted proton beam in 2012.

A superconducting isochronous cyclotron C400 has been designed by the IBA–JINR collaboration. This cyclotron will be used for radiotherapy with proton, helium and carbon ions. The $^{12}\text{C}^{6+}$ and $^4\text{He}^{2+}$ ions will be accelerated to an energy of 400 MeV/amu, the protons will be extracted at the energy 265 MeV. The construction of the C400 cyclotron was started in 2010 within the framework of the Archarde project (France).

Development of spectrometric CT tomographs may allow one to determine the chemical composition of a substance together with the density, measured using traditional CT. This may advance modern diagnostic methods significantly. JINR develops fundamentally new pixel detector systems for spectrometric CT.

The time-of-flight (TOF) system installed in the positron emission tomograph (PET) permits essential reduction in the detector noise from occasional events of different positron annihilations. The micropixel avalanche photodiodes (MAPDs) developed at JINR allow a factor of 1.5 reduction in the resolution time for the PET TOF system and suppression of the noise level as compared to commercial PET. The development of a combined PET/MRI is of considerable medical interest, but it cannot be made with the existing PET tomographs based on detectors of compact photomultipliers due to strong alternating magnetic field of MRI. Change-over to detectors of micropixel avalanche photodiodes permits making a combined PET/MRI.

В Лаборатории ядерных проблем им. В. П. Дзепелова ОИЯИ ведутся прикладные исследования в области радиационной медицины, включающие в себя 3-мерную конформную протонную терапию, разработку ускорительной техники для протонной и углеродной терапии, развитие новых типов детекторных систем для спектрометрического компьютерного томографа (КТ) и позитронно-эмиссионного томографа (ПЭТ).

ОИЯИ совместно с бельгийской фирмой ИВА осуществил разработку специализированного медицинского циклотрона С235-V3 для протонной терапии. В настоящее время изготовлены все основные системы циклотрона. В 2011 г. планируется провести его сборку в ОИЯИ, а в 2012 г. — его испытания с выведенным протонным пучком.

Сверхпроводящий изохронный циклотрон С400, предназначенный для углеродной терапии, разработан совместно ОИЯИ и ИВА. Этот циклотрон будет использоваться для радиотерапии протонами, ионами гелия и ионами углерода. Ионы углерода и гелия будут ускорены до энергии 400 МэВ/нуклон, а протоны выведены из циклотрона при энергии 265 МэВ. Изготовление циклотрона С400 начато в 2010 г. в рамках проекта «Archarde» (Франция).

Разработка спектрометрического КТ позволит определять химический состав исследуемого вещества наряду с его плотностью, измеряемой с помощью стандартных КТ. Это может обеспечить существенное развитие методики и возможностей компьютерной томографии. ОИЯИ разрабатывает принципиально новый полупроводниковый пиксельный детектор на основе GaAs(Cr) для спектрометрического КТ.

Времяпролетная система ПЭТ значительно сокращает количество ложных срабатываний его детекторной системы, возникающих от разных аннигиляционных событий. Микропиксельный фотодиод, разрабатываемый в ОИЯИ, позволяет в 1,5 раза увеличить времяпролетное разрешение и, соответственно, значительно снизить уровень шумов по сравнению с коммерческими ПЭТ. Разработка совмещенного ПЭТ/МРТ томографа представляет значительный интерес для практической медицины. Такой томограф не может быть изготовлен на основе фотоумножителей — современной детекторной базе ПЭТ. Использование микропиксельных фотодиодов позволяет решить эту проблему и создать совмещенный ПЭТ/МРТ томограф.

PACS: 87.56.-v; 87.64.-t; 87.80.-y

PROTON THERAPY

Dubna is one of the leading proton therapy research centers in Russia [1]. The JINR Medico-Technical Complex (MTC) consists of seven rooms, where proton, pion and neutron beams are used [1–3]. The research synchrocyclotron with a proton energy of 660 MeV and current of 3 μ A has been used for medical applications since 1967. The modern technique of 3D conformal proton radiotherapy was first effectuated in Russia at this center, and now it is effectively used in regular treatment sessions [1–3]. The irradiated dose distribution in 3D conformal proton therapy coincides with the tumor target shape with an accuracy of 1 mm. This required solving the following tasks: formation and monitoring of proton beams with the required parameters; development of the computer codes and a technique for construction



Fig. 1. Proton therapy in medical cabin 1 of JINR MTC

Table 1. Diseases treated at JINR by the proton medical beams in 1999–2010

Disease	Number of patients
Meningioma	118
Chordoma, chordosarkoma	21
Glioma	45
Acoustic Neurinoma	9
Astrocytoma	27
Paraganglioma	5
Pituitary Adenoma	21
AVM	62
Brain and other metastase	56
Other head and neck tumors	175
Melanoma	11
Skin diseases	43
Carcinoma metastase of the lung	9
Breast cancer	46
Prostate Adenoma	1
Sarcoma	13
Others	25
Total	687

of individual collimators and boluses; development of a system for immobilization of the patient and verification of its position relative to the proton beam. The equipment used for 3D conformal therapy in room 1 is presented in Fig. 1. About 100 patients undergo a course of fractionated treatment here every year. About 700 patients were treated by proton beams during the last 10 years (Table 1).

PROTON CYCLOTRON C235-V3

The C235-V3 cyclotron, superior in its parameters to the IBA C235 medical proton cyclotron installed in 10 proton treatment centers of the world, has been designed and manufactured by the JINR–IBA collaboration. This cyclotron is an essentially modified version of IBA C235 cyclotron [4, 5] (Table 2).

One of the goals is to modify the sector spiral angle at $R > 80$ cm for improving the cyclotron working diagram (Fig. 2) and reducing of coherent beam losses at acceleration. The coherent beam displacement z from the median plane is defined by the vertical betatron tune Q_z : $z \propto Q_z^{-2}$. At $Q_z \approx 0.2$ the coherent beam displacement corresponds to 7 mm and at the free axial oscillation amplitude of 2–3 mm can cause beam losses due to reduction of the sector gap in the C235 cyclotron. An increase of the vertical betatron tune from $Q_z \approx 0.2$ – 0.25 to $Q_z \approx 0.4$ in C235-V3 permits the coherent losses at proton acceleration to be reduced by a factor of 3–4 (Table 2).

Modification of the extraction system is another aim of the new C235-V3 cyclotron [4]. The main peculiarity of the cyclotron extraction system is a rather small gap (9 mm) between the sectors in this area. The septum surface consists of several parts of circumferences of different radii. The septum thickness is linearly increased from 0.1 mm at the entrance to 3 mm at the exit. The proton extraction losses essentially depend on the septum geometry. In

Table 2. JINR-IBA C235-V3 cyclotron

Parameter	C235	C235-V3
Optimization of magnetic field at modification of sector		Modification of sector azimuthal angle at $R > 80$
Vertical betatron frequency at $R > 80$	$Q_z = 0.25$	$Q_z = 0.45$
Vertical coherent beam displacement related to median plate effects, mm	6-7	1.5-2
Beam losses at proton acceleration, %	50	15
Beam losses at extraction, %	50	25
Reduction of radiation dose of cyclotron elements		2-3 times

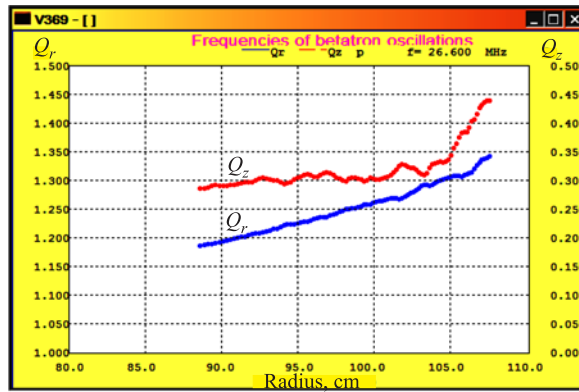


Fig. 2. Dependence of betatron tunes on radius in the C235-V3 cyclotron

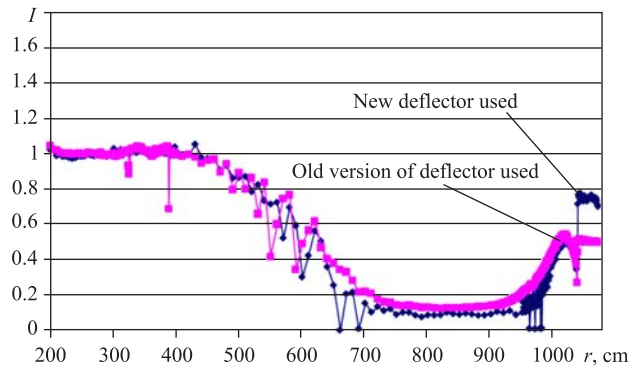


Fig. 3. Proton beam extraction in the C235 cyclotron with old IBA deflector and new electrostatic deflector developed at JINR

the septum geometry proposed at JINR, where the minimum of the septum thickness is placed at a distance of 10 cm from the entrance, the losses were reduced from 25 to 8%. Together with the optimization of the deflector entrance and exit positions, it leads to an increase in the extraction efficiency to 80%. The new extraction system was constructed and tested at the IBA C235 cyclotron. The experimentally measured extraction efficiency was improved from 60% for the old system to 77% for the new one (Fig. 3).

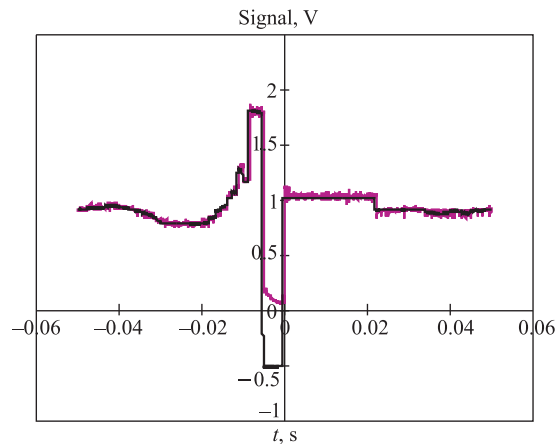


Fig. 4. Beam intensity variation at the IBA C235 proton cyclotron

Advantages of the medical proton cyclotron are simplicity, reliability, small size, and, most importantly, the ability to modulate rapidly and accurately the proton beam current (Fig. 4). The current modulation of the extracted proton beam at a frequency of up to 1 kHz [5] is most advantageous with Pencil Beam Scanning and Intensity Modulated Proton Therapy. The energy of the extracted beam in the cyclotron is fixed. However, the fast proton energy variation at a rate of 15 MeV/s is easily performed during active cancer treatment by using a wedge degrader. This energy variation rate is faster than in the typical synchrotron regime.

SUPECONDUCTING CYCLOTRON C400 APPLIED FOR CARBON THERAPY

Carbon therapy is the most effective method to treat resistant tumors. A compact superconducting isochronous cyclotron C400 (Fig. 5) was designed by the JINR–IBA collaboration (Table 3) [5–9]. This cyclotron will be used for radiotherapy with protons, helium and carbon ions. The $^{12}\text{C}^{6+}$ and $^4\text{He}^{2+}$ ions will be accelerated to an energy of 400 MeV/amu and H_2^+ ions will be accelerated to an energy of 265 MeV/amu, and protons will be extracted by stripping.

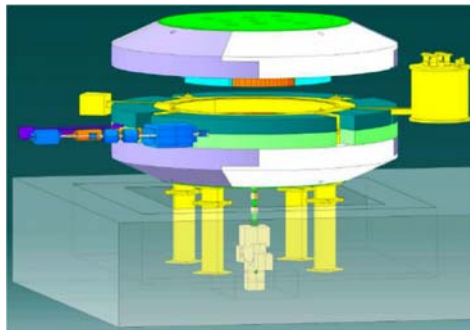


Fig. 5. General view of the C400 cyclotron

Table 3. Main parameters of the C400 cyclotron

General properties	
Accelerated particles	H_2^+ , $^4He^{2+}$, $^6Li^{3+}$, $^{10}B^{5+}$, $^{12}C^{6+}$
Injection energy, keV/Z	25
Final energy of: ions protons	400 MeV/amu 265 MeV
Extraction efficiency, %	~ 70 (by deflector)
Number of turns	~ 1700
Magnetic system	
Total weight, t	700
Outer diameter, m	6.6
Height, m	3.4
Pole radius, m	1.87
Valley depth, cm	60
Bending limit	$K = 1600$
Hill field, T	4.5
Valley field, T	2.45
RF system	
Radial dimension, cm	187
Vertical dimension, cm	116
Frequency, MHz	75
Operation	4 harmonic
Number of dees	2
Dee voltage, kV:	
center	80
extraction	170

Three external ion sources will be mounted on the switching magnet in the injection line located below the cyclotron. The $^{12}C^{6+}$ ions are produced by a high-performance ECR at an injection current of $3 \mu A$. The alphas are produced by the other ECR source, while H_2^+ are produced by a multicusp ion source. All species have a Q/M ratio of $1/2$.

The dee tips have the vertical aperture 1.2 cm in the first turn and 2 cm in the second and subsequent turns. In the first turn the gaps were delimited with pillars reducing the transit time. The azimuth extension between the middles of the accelerating gaps was chosen to be 45° . The electric field in the inflector was chosen to be 20 kV/cm. Thus, the height (electric radius) of the inflector is 2.5 cm. The gap between the electrodes was taken to be 6 mm, and the tilt parameter is $k' = 0.1$. The aspect ratio between the width and the spacing of the electrodes was taken to be 2 to avoid the fringe field effect.

The 3D TOSCA simulation (Fig. 6) and the design of the C400 magnetic system were based on the main characteristics of the cyclotron: four-fold symmetry and spiral sectors; deep-valley concept with RF cavities placed in the valleys; elliptical pole gap decreasing from 120 mm at the center to 12 mm at the extraction; proton acceleration up to a distance of 10 mm from the pole edge to facilitate extraction; pole radius 187 cm; hill field 4.5 T, valley field 2.45 T; magnetic induction inside yoke less than 2–2.2 T; the magnet weight 700 tons and the magnet yoke diameter 6.6 m; the main coil current 1.2 MA. The sectors are designed with a flat top surface and without additional grooves, holes, etc. The sectors

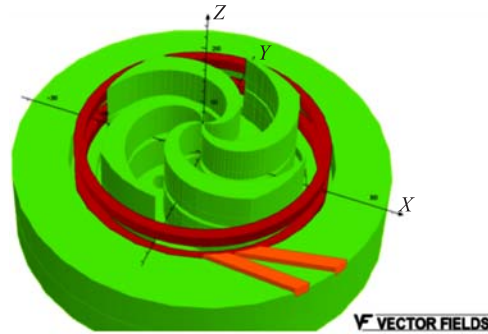


Fig. 6. 3D TOSCA simulation of the C400 magnetic system

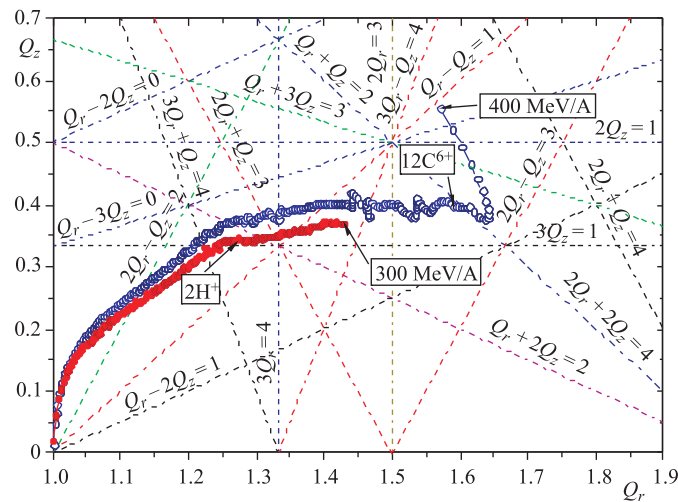


Fig. 7. Working diagram of the cyclotron

have the following parameters: the initial spiral law with $N\lambda = 77$ cm with increasing spiral angle to the final radius with $N\lambda \sim 55$ cm; the sector azimuth width is varied from 25° at the cyclotron center to 45° at the sector edge; the axial profile is the ellipse with the 60/1874 mm semi-axis, at the final radii axial profile of the ellipse is cut by the planes at the distance $z = \pm 6$ mm. The optimized sector geometry provides vertical focusing $Q_z \sim 0.4$ in the extraction region (Fig. 7).

Acceleration of the beam will occur at the fourth harmonic of the orbital frequency, i.e., at 75 MHz. The acceleration will be obtained through two cavities placed in the opposite valleys. Two 45° dees working at the fourth harmonic will guarantee the maximum acceleration. The dee voltage increases from 80 kV at the center to 170 kV in the extraction region. A geometric model of the double gap delta cavity housed inside the valley of the magnetic system was developed in the Microwave Studio. The depth of the valley permits accommodation of the cavity with total height 116 cm. The vertical dee aperture was equal to 2 cm. The accelerating gap was 6 mm at the center and 80 mm in the extraction region. The distance between the dee and the backside of the cavity was 45 mm. The azimuth extension of the cavity (between the

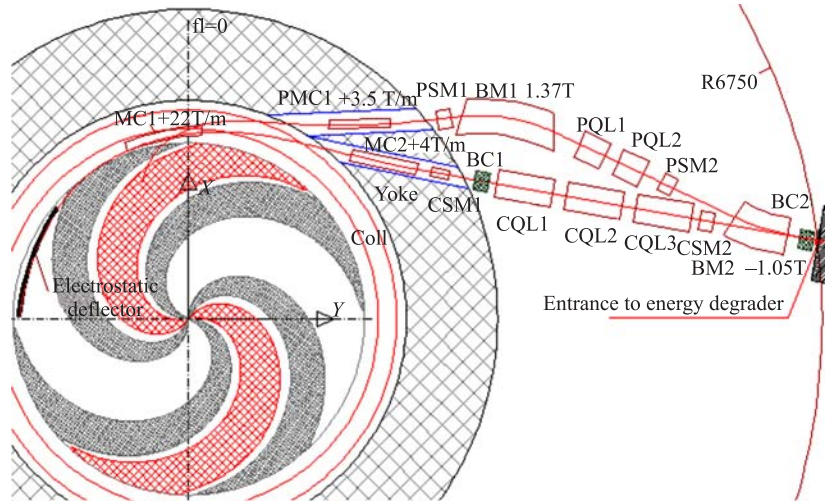


Fig. 8. Layout of the C400 cyclotron with two extraction lines

middles of the accelerating gaps) was 45° up to the radius 150 cm. The cavities have a spiral shape similar to the shape of the sectors. We inserted four stems with different transversal dimensions in the model and investigated different positions of the stems to ensure increasing voltage along the radius. The thickness of the dee was 20 mm. The edges of the dees are 10 mm wide. Based on the 2D electric field simulations, we have chosen the optimal form of the dee edges. RF heating simulation was performed to determine the cooling system layout.

During the whole range of acceleration the carbon beam crosses the lines of 15 resonances up to the 4th order. The working diagrams presented in Fig. 8 were computed via the analysis of the small oscillations around the closed orbits. All resonances can be subdivided into two groups. The first group consists of six internal resonances ($nQ_r \pm kQ_z = 4$, $n, k = 0, 1, 2, 3, 4$, $n + k \leq 4$) having the main 4th harmonic of the magnetic field as a driving term. The second group includes 11 external resonances ($nQ_r \pm kQ_z = m$, $m = 0, 1, 2, 3$) that could be excited by the magnetic field perturbations.

Extraction of protons is supposed to be done by means of the stripping foil. It was found that 265 MeV is the minimal energy of protons for two-turn extraction. The radius of the foil in this case is 161.3 cm, and the azimuth is 51° .

It is possible to extract the carbon beam by means of one electrostatic deflector (which is located in the valley between the sectors) with a 150 kV/cm field inside. The septum of the deflector was located at the radius 179.7 cm for tracking simulation. The extraction efficiency was estimated at 73% for the septum with increased 0.1–2 mm thickness along its length. The extraction of the carbon and proton beams through the separate channels and their further alignment by the bending magnets outside the cyclotron was chosen as an acceptable option. The passive magnetic elements (correctors) are supposed to be used inside the cyclotron and the active current elements (quadrupole lenses and bending magnets) outside the yoke. A schematic view of both lines is shown in Fig. 8. It is possible to align both beams in one direction just in front of the energy degrader (6750 mm from the cyclotron center). Both beams have a spot with $\sigma_{x,y} < 1$ mm at this point. Transverse emittances are 10π mm · mrad and 4π mm · mrad for the extracted carbon beam.

DETECTORS FOR TOMOGRAPHY

Development of spectrometric computer tomographs (CT) may allow one to determine chemical composition of a substance together with the density, measured using traditional CT. The main idea is to use peculiarities of X-ray absorption spectra near the K-edge lines, which are individual for different chemical elements and can be measured by the spectrometric detectors. Using this additional information may greatly improve existing diagnostic techniques.

The gamma-ray energy in the spectral CT based on the JINR-TSU GaAs pixel detector [10] (Fig. 9) is determined by a special chip developed by Medipix collaboration [11] which is capable of registering gamma quanta in selected energy range, thus implementing color X-ray imaging.

The detecting systems of the spectrometric CT are based on the semiconducting heterostructures. Together with spectrometric possibilities, the pixel detectors on the basis of GaAs(Cr) have a high spatial resolution ($\sim 100 \mu\text{m}$), their sensitivity is an order of magnitude better as compared with Si detectors at a photon energy of 30–35 keV (Fig. 10).



Fig. 9. Spectrometric detector on the basis of GaAs(Cr) pixel sensor with 256×256 channels of $50 \mu\text{m}$ resolution and Medipix chip

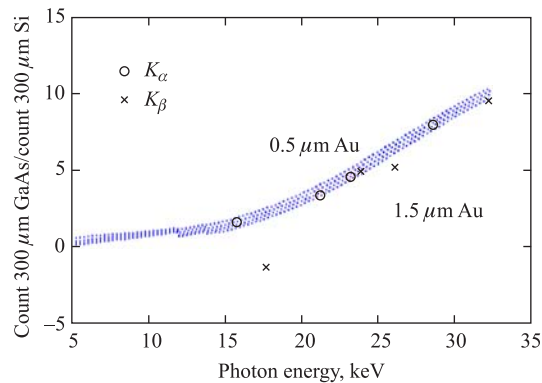


Fig. 10. Dependence of count ratios of GaAs(Cr) and Si detectors on the photon energy

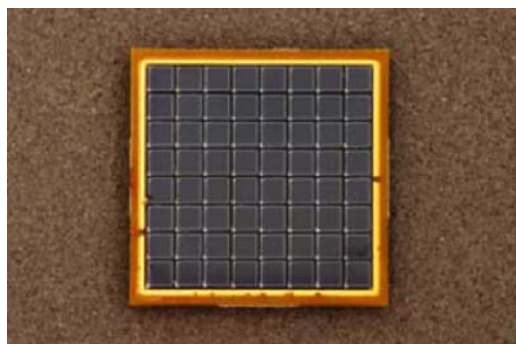


Fig. 11. Micropixel avalanche photodiodes

Another approach is used to improve existing detector systems for PET. The micropixel avalanche photodiode (MAPD) consists of many microcells, each working in the yes/no Geiger mode with a high internal gain (up to 10^6) and being capable of detecting single photons. The MAPD pixel size is 2–30 μm . The MAPD advantages over photomultipliers (PM) [12] are photon detection efficiency up to 30%; insensitivity to magnetic field; compactness and rigidity; low voltage supply ($< 100\text{ V}$). In comparison with other solid-state photodetectors based on micropixels, the advantages are high dynamic range, high gain and better radiation hardness.

MAPDs are more and more widely *inculcated* in nanoindustry (laser location, optical-fiber communication, optical information transmission lines, systems for optical readout of super-high-density information from various carriers on the nanostructure basis, luminescence of quantum dots) and in development of medical diagnosis equipment (PET, TOF-PET, combined PET/MRI).

The detector matrix (Fig. 11) was constructed by the JINR–Zecotec collaboration for PET on the basis of the depth MAPD-3N-1P and LFS scintillator crystals with 64 (8×8 matrix) electronic channels. The LFS crystals measure $3.5 \times 3.5 \times 15\text{ mm}$. These crystals provide higher light conversion efficiency and faster light response in comparison with the LSO crystals. The MAPD-3N-1P+LFS detector matrix has the same advantages as the detector on the basis of the multichannel PM: the noise in one channel does not affect another channel, the uniformity of the pixel parameters in the matrix is around 10%, which corresponds to 50% for different channels of the photomultiplier.

The PET is especially advantageous in study of dynamics of metabolic processes. However, the PET coordinate resolution is a few times worse than resolution obtained using CT or MRI. The PET coordinate resolution is influenced by several factors: the positron deceleration length before annihilation, the noncollinearity of X rays (about 4 mrad) due to the positron momentum, the detector space resolution and the uncertainty of depth of the photon interaction in the scintillation crystal.

The basic aim of the PET detector system is measurement of photon parameters from one positron annihilation event, minimization of occasional coincidences in detection of photons from different annihilation events, and reduction of influence of scattering effects for photons.

The new PET based on the time-of-flight (TOF) technique permits suppression of occasional coincidence of gamma rays produced in different annihilation processes. The accurate measurement of times in detection of both annihilation photons permits the positron annih-

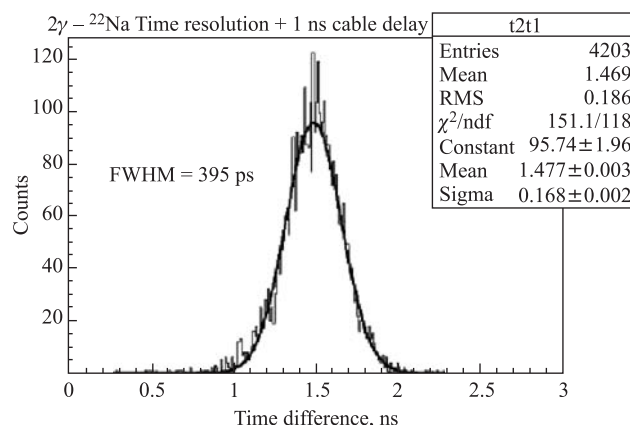


Fig. 12. Time resolution of two MAPD-3N-1P+LFS detectors for photo pick events

lation coordinate to be found. However, in present PET the time resolution corresponds to 600–800 ps. It is determined by several factors: the scintillator and detector time response, the depth of photon interaction in the crystal, the light reflection effects in the crystal, etc. However, the present PET time resolution of 600 ps essentially suppresses the occasional events in detection of two gamma rays produced in different positron annihilation events. The resolution time of the MAPD-3N-1P+LFS detector is about 400 ps (Fig. 12), a factor of 1.5 times lower than in modern PET tomographs. It permits a factor of 1.5 lower multiplicative reduction coefficient (noise level from occasional events).

A combined PET/MRI tomograph is under consideration in many research centers. The key problem in construction of a combined PET/MRI tomograph is associated with the PET photodetector operating in a high MRT magnetic field. The photomultipliers used in the present PETs are not suitable for a combined PET/MRI because none of them can work in a high MRI magnetic field. Micropixel avalanche photodiodes (Fig. 11) allow making a combined PET/MRI tomograph.

CONCLUSION

We have reported numerous spin-offs for radiation medicine from technological development of accelerator techniques and detector systems performed at DLNP during the last few years. This applied activity is oriented towards the development of 3D conformal proton therapy, accelerator techniques for proton and carbon treatments and new types of detector systems for tomography.

The method of 3D conformal irradiation of deep-seated tumors with a proton beam was implemented at DLNP for the first time in Russia and is effectively used today for cancer treatment here. About 700 patients were treated by proton beams during the last 10 years.

Proton therapy hospital centers have become wide-spread in the world during the last decade. The medical cyclotron C235-V3 intended for hospital centers of proton therapy was developed by the JINR-IBA collaboration. We plan to assemble this cyclotron at JINR in 2011 and perform tests with the extracted proton beam in 2012. The first medical cyclotron C235-V3 will be installed in the Dimitrovgrad hospital center of proton therapy.

Carbon therapy is the most effective method to treat radioresistant tumors. A compact superconducting cyclotron C400 has been designed by the JINR–IBA collaboration. This cyclotron will be used for radiotherapy with proton, helium and carbon ions. The construction of C400 was started in 2010 within the framework of the Archarde project in Caen (France).

GaAs(Cr) pixel detectors developed at DLNP are promising for application in medical imaging since they allow routine measurements of the energy of X-ray photons. Development of the spectrometric tomography based on such detectors can help in determining chemical composition of a substance in addition to the density measured by traditional CT.

High time resolution has become important for TOF-PET where improved signal-to-noise ratio images, lower exposure rates and faster image reconstruction are required. A resolution of about 400 ps (FWHM) was obtained in our measurements of LFS–MAPD detectors.

PET/MRI will combine the good sensitivity of PET with the variety of contrast mechanisms for anatomical and functional imaging of MRI. To enable PET inside MRI it is suitable to replace the photomultipliers used in PET by the MAPD which are insensitive to the magnetic field of MRI.

Acknowledgements. The development of GaAs(Cr) semiconductor detectors was performed at support of the Russian Foundation for Basic Research, grant 09-99028-r-ofi.

REFERENCES

1. Savchenko O. V. 40 Years of Proton Therapy on Synchrocyclotron and Phasotron of LNP, JINR // J. Med. Phys. 2007. No. 3–4.
2. Agapov A. V. et al. Technique of 3D Conformal Proton Therapy // Part. Nucl., Lett. 2005. V. 2, No. 6(129). P. 80–86.
3. Shvidky S. V. et al. Proton Three-Dimensional Radiotherapy and Radiosurgery of Intracranial Targets in Dubna // Radioprotection. 2008. V. 43, No. 5. P. 7.
4. Karamysheva G. et al. Simulation of Beam Extraction from C235 Cyclotron for Proton Therapy // Part. Nucl., Lett. 2010. V. 7, No. 4.
5. Syresin E. M. Centers of Hadron Therapy on the Basis of Cyclotrons // RUPAC 08. Zelenograd, 2008. P. 316.
6. Jongen Y. Design of a $K = 1600$ SC Cyclotron for Carbon Therapy // ECPM. Nice, 2006. P. 30.
7. Jongen Y. et al. Design Studies of the Compact Superconducting Cyclotron for Hadron Therapy // EPAC 06. Edinburgh, 2006. P. 1678.
8. Jongen Y. et al. IBA C400 Cyclotron Project for Hadron Therapy // Cyclotrons. Italy, 2007. P. 151.
9. Jongen Y. et al. Current Status of the IBA C400 Cyclotron Project for Hadron Therapy // EPAC 08. Venice, 2008. P. 1806.
10. Tlustos L., Chelkov G., Tolbanov O. Characterization of GaAs(Cr) Medipix2 Hybrid Pixel Detectors // Proc. of iWoRid. Prague, 2009.
11. Llopert X., Campbell M. First Test Measurements of a 64k Pixel Readout Chip Working in Single-Photon Counting Mode // Nucl. Instr. Meth. A. 2003. V. 509. P. 157–163.
12. Sadygov Z. et al. Three Advanced Designs of Micro-Pixel Avalanche Photodiodes: Their Present Status, Maximum Possibilities and Limitations // Nucl. Instr. Meth. A. 2006. V. 567. P. 70–73.

Received on November 1, 2010.